Rapid and Versatile Synthesis of Glutathione-Responsive Polycarbonates from Activated Cyclic Carbonates

Xiao Zhang,<sup>a</sup> Bowen Zhao,<sup>a</sup> Shiwei Fu,<sup>a</sup> Ronald S. Seruya,<sup>a</sup> John F. Madey III,<sup>a</sup> Eva Bukhryakova,<sup>a</sup> and Fuwu Zhang\*<sup>a,b</sup>

<sup>a</sup>Department of Chemistry, University of Miami, 1301 Memorial Drive, Coral Gables, Florida, 33146, United States. Email: fxz174@miami.edu. <sup>b</sup>The Dr. John T. Macdonald Foundation Biomedical Nanotechnology Institute, University of Miami, 1951 NW 7th Ave, Miami, Florida, United States, 33136

KEYWORDS. Disulfide, drug delivery, nanomaterial, nanomedicine, polycarbonate.

ABSTRACT. Aliphatic polycarbonates (APCs) are promising biocompatible and degradable polymers with immense potential for biomedical applications. However, current synthetic approaches to stimuli-responsive APCs remain limited and often complicated requiring multiple-step postpolymerization reactions. To address these limitations and unlock the full potential of APCs in the development of advanced biomaterials, we developed a rapid and versatile strategy to synthesize glutathione-responsive polycarbonates through the controlled ring-opening polymerization of cyclic carbonates with activated disulfides. Responsive pendent moieties could

be easily introduced in one step through a highly efficient thiol-disulfide exchange reaction enabled by the reactive pyridyl disulfides, providing a simple and versatile approach to fine-tuning polymer's physiochemical properties for biomedical applications. As a proof of concept, we prepared an amphiphilic glutathione (GSH)-responsive polycarbonate-drug conjugate by initiating the activated cyclic carbonate monomer with methyl polyethylene glycol and then conjugating the anticancer drug mertansine via the thiol-disulfide exchange reaction. The self-assembled nanoparticles were a smart drug delivery system with GSH-triggered drug release specifically within cancer cells and a remarkable selective toxicity toward cancer cells over healthy cells, showcasing the exceptional promise of this GSH-responsive polycarbonate for biomedical applications.

## 1. Introduction

Cancer is a substantial global healthcare concern and currently stands as the second leading cause of death in the United States, characterized by notably elevated rates of both incidence and mortality. Chemotherapy that employs drugs to kill active cancer cells noninvasively remains the most common methods for cancer therapy. However, many therapeutic agents, either small-molecule drugs or biologic agents, have been challenged by their lack of specificity, short half-life, low therapeutic efficiency, increased risk of undesired side effects, and requirements of higher-dose and frequent administration. There is pressing need for biocompatible and degradable smart drug delivery systems (SDDSs) that can preferentially accumulate and bind to diseased sites with controlled drug release.

Aliphatic polycarbonates (APCs) are a class of polymers that feature a backbone comprising of repeating carbonate (-O-C(O)-O-) linkages without aromatic groups between repeating carbonate

units. 15 APC can be broken down into non-toxic small molecules in vivo and eliminated through natural metabolic pathways. 16 The biodegradability, together with low immunogenicity and cytotoxicity, render them as promising candidates for medical and biological applications over traditional synthetic polymers. 17-19 The stimuli-responsive APCs, which can take advantage of the different biological conditions (such as temperature, pH, enzyme concentration, etc.) occurring in pathological tissues versus in normal tissues to trigger the selective release of therapeutic agents, are particular attractive as highly efficient SDDSs with great potential of increased bioavailability, prolonged blood circulation time, preferential accumulation in targeted tissues, reduced side effects, and improved overall therapeutic efficacy. 20-22 The disulfide bond (-S-S-) is labile in the presence of overexpressed glutathione (GSH) through thiol-disulfide exchange reactions, leading to triggered release of cargoes in cancerous cells, while remaining stable under normal low GSH conditions during extracellular circulation in vivo. 23-24 This property make its introduction to polymeric networks as redox-responsive linkers has become an attractive strategy to build dynamic covalent materials with stimuli-responsiveness.<sup>25-30</sup> Polymerization of activated disulfide monomers to afford polymers with pendant activated disulfide is particularly attractive as the activated disulfides are highly reactive towards thiols and could be readily used to install labile functionalities, induce crosslinking, and conjugate drug molecules. For example, Zhuang and Thayumanavan synthesized GSH-responsive polymers through the reversible addition fragmentation chain transfer (RAFT) polymerization of activated methacrylate monomers, where the pendant activated disulfides were used to crosslink the micellar structure (Scheme 1A).<sup>31</sup> Barz developed polypeptides *via* the ring-opening polymerization (ROP) of reactive monomer S-ethylsufonyl-l-cysteine N-carboxy anhydride (NCA). The obtained polypeptide could chemoselectively react with thiols for the

postpolymerization of disulfide formation (Scheme 1A).<sup>32-33</sup> However, this intriguing approach in polycarbonates has not been reported, where the activated disulfide may react with the initiator in the presence of catalysts causing premature crosslinking and other unwanted ring-open reaction during polymerization.

Herein, we reported a simple and efficient synthetic method to synthesize well-defined pyridyl disulfide-functionalized polycarbonates *via* the ROP of activated cyclic carbonates (Scheme 1B). Benefiting from the inherently highly reactive nature of the pyridyl-disulfide group towards thiols, a wide range of functional moieties, including neutral hydrophilic methyl ether, amines, carboxylic acids, and zwitterionic amino acids, were successfully conjugated to reactive polycarbonates through thiol-disulfide exchange reactions, yielding a series of advanced GSH-responsive multifunctional APCs. The versatility of the activated pendent side chains was further demonstrated by conjugating a thiol-containing highly cytotoxic drug mertansine (DM1) as a model therapeutic agent to a polyethylene glycol (PEG)-initiated activated APC, which self-assembled into micellar nanoparticles for triggered drug release.

# (A) Previous strategies

RAFT polymerization of activated methacrylates

· ROP of activated NCAs

## (B) Our strategy

· ROP of activated cyclic carbonates

**Scheme 1.** (A) Reported strategies for activated polymer synthesis by the RAFT polymerization of activated methylacrylate<sup>31</sup> and ROP of activated NCAs.<sup>32-33</sup> (B) Syntheses of activated polymers **Bn-PCssPy** *via* cyclic carbonate monomer **CssPy**, and their postmodification *via* thiol-disulfide exchange reactions.

# 2. Results and Discussion

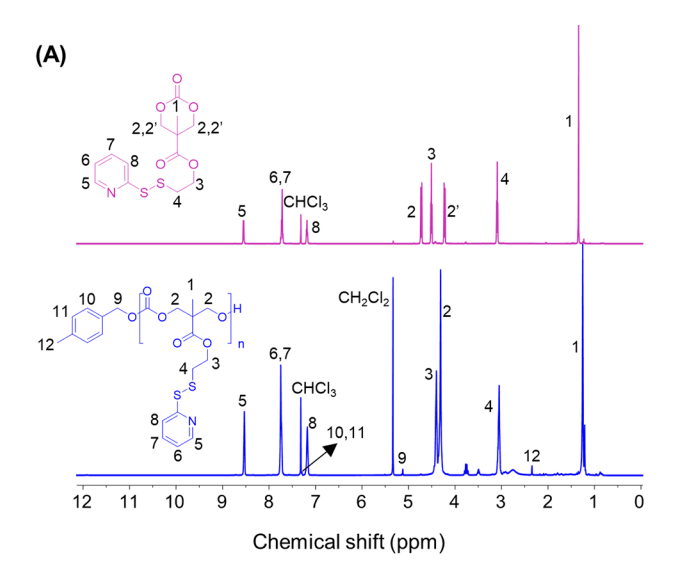
**2.1. Monomer synthesis.** The monomer, 2-(pyridin-2-yldisulfanyl)ethyl 5-methyl-2-oxo-1,3-dioxane-5-carboxylate (**CssPy**), a six-membered cyclic carbonate with a pyridyl disulfide group, was synthesized *via* an improved two-step synthetic route (Scheme 1B). Tommercially available 2,2-bis(hydroxymethyl)propionic acid (bis-MPA), an important intermediate in petrochemical manufacturing, was employed as the starting material for monomer preparation. The cyclic carbonate intermediate with an active pentafluorophenyl ester (1) was first obtained with a yield of 61% from a 24-hour reaction of bis-MPA with 2.5 equivalents of

bis(pentafluorophenyl)carbonate in the presence of cesium fluoride (CsF) in anhydrous tetrahydrofuran (THF). The cyclic carbonylation of the 1,3-diol and transformation of carboxylic acid into a pentafluorophenyl ester group could be completed simultaneously in this one-pot reaction. The pentafluorophenyl ester group of 1 was then substituted with a pyridyl disulfide moiety by reaction with 2-(pyridin-2-yldisulfanyl)ethanol (2) in anhydrous THF and purified by silica gel column chromatography, giving the activated cyclic carbonate monomer CssPy in 63% isolated yield. The intermediates and monomer CssPy have been characterized by proton nuclear magnetic resonance (<sup>1</sup>H NMR) and electrospray ionization mass spectrometry (ESI-MS) analyses (Figure S1-S6). The ring-structure of monomer CssPy was confirmed by the larger chemical shift difference between the two doublet peaks that corresponded to the diastereotopic methylene protons (labeled as 2 and 2' in Figure S7) and their more downfield positions in the <sup>1</sup>H NMR spectrum compared to those of bis-MPA (Figure S7). This was mainly because the asymmetric chemical environments of the methylene protons were significantly magnified due to the rotational rigidity after ring-closing. The peaks located at 8.45, 7.85, and 7.12 ppm indicated the successful incorporation of pyridine ring into the carbonate monomer (labeled as proton 5-8 in Figure S7). Compared to common synthetic route for cyclic carbonates that involved the functionalization of carboxylic acid under acidic or basic conditions and cyclization with phosgene or similar alternatives, this improved synthetic route featured easy purification with a high yield and avoided the use of highly toxic phosgene, greatly reducing the difficulty and hazard during the synthesis process.<sup>34</sup>

# **2.2. Polymerization of Pyridine Disulfide-Containing Cyclic Carbonate Monomer.**Anionic ROP of six-membered cyclic carbonates is a preferred method for the controlled preparation of well-defined polycarbonates under milder conditions.<sup>35-37</sup> In this study, different

reaction conditions have been investigated for the ROP of pyridyl disulfide-containing cyclic carbonate monomer CssPv (Scheme 1B and Table 1) in the presence of organocatalyst 1,8diazabicyclo[5.4.0]undec-7-ene (DBU), which has shown excellent catalytic ability in the ROP of cyclic carbonate monomer. 17,38 The monomer concentration was maintained at 0.5 M in anhydrous dichloromethane, with DBU concentration at 1 equivalent to the initiator. 4methylbenzyl alcohol was used to initiate the ROP with varied monomer-to-initiator molar ratios  $([M]_0/[I]_0)$ . After reacting for 2 hours at room temperature, the reaction mixture was quenched by addition of excessive amount of acetic acid. The polymer was facilely purified three times by washing with diethyl ether-hexane mixed solution (1/1, v/v) to remove the unreacted monomer and catalyst, giving **Bn-PCssPy**. The obtained polymers were characterized by <sup>1</sup>H NMR spectroscopy (Figure 1A and S8-S12) and size-exclusion chromatography (SEC) (Figure 1B). Significant changes were observed between the monomer and polymer in <sup>1</sup>H NMR spectra. Two distinct doublet peaks of diastereotopic methylene protons (labeled as 2 and 2' in Figure 1A) at 4.67 ppm and 4.19 ppm were observed in the monomer CssPy but diminished after polymerization and resulted in a merged broad peak at 4.38 ppm in the <sup>1</sup>H NMR. Likewise, the splitting peaks of the monomer, including protons 4-8, also transitioned broader after the polymerization (Figure 1A). When  $[M]_0/[I]_0 = 20$ , the polymerization could reach almost 100% conversion within 2 hours at room temperature. The value of number-averaged molar mass ( $M_n$  = 6.7 kDa) and degree of polymerization (DP = 20) were estimated by the integral ratios of the methylene protons connected to oxygen (proton 2 and 3, resonating between 4.36 to 4.27 ppm) to the methyl protons of the initiator at the  $\alpha$ -chain end (proton 12, resonating at 2.32 ppm). Then varied [M]<sub>0</sub>/[I]<sub>0</sub> feed ratios (10, 20, 30, 50, and 100) was investigated systematically using the same reaction condition to tune the polymer backbone length (Table 1). It was found that both

 $M_{\rm n}$  and DP increased in accordance with the feed ratios. Improved yields with the feed ratios were also noticed attributed to the decreased solubility of the larger polymers in the hexanediethyl ether mixed solution. The increased  $[M]_0/[I]_0$  ratios also resulted in a slightly decreased conversion and broadening distribution of molecular mass. When  $[M]_0/[I]_0 = 100$ , the polymerization reached a 70% of conversion and 1.25 of dispersity (D) (Figure 1B) in 2 h at room temperature. The polymerizations of the activated disulfide-containing monomer proceeded in a controlled fashion and had the potential to be applied for the tunable synthesis of polycarbonates for different applications. Polymerization at a lower temperature was also attempted (Table 1). The reaction rate was significantly slowed down when the temperature was lowered to 0 °C, resulting in low conversions (< 50%) and yields (< 30%) even after a longer reaction time (4 h). Furthermore, we conducted thermogravimetric analysis (TGA) of these GSH-responsive polycarbonates under nitrogen atmosphere with a heating rate of 10 °C/min. Bn-PCssPy of different lengths showed no significant weight changes observed below 170 °C, and two stages of decomposition that lead to approximately 85% and 7% mass loss were observed at 170-280 °C and 400-520 °C, respectively (Figure S14 and Table S1).



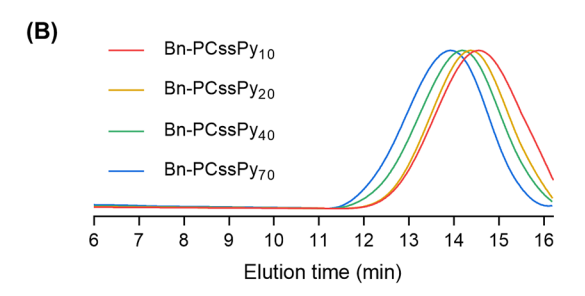


**Figure 1.** (A) Comparison of <sup>1</sup>H NMR spectra between the monomer **CssPy** and polymer **Bn-PCssPy** in CDCl<sub>3</sub>. (B) Normalized SEC traces of **Bn-PCssPy** with different degrees of polymerization.

**Table 1.** Ring-opening polymerization of the activated cyclic carbonate monomer under different conditions.

Entry	Mono mer <sup>b</sup>	T (°C)	[M] <sub>0</sub> /[I] <sub>0</sub>	Time (h)	Conver sion <sup>c</sup> (%)	$DP^d$	M <sub>n, NMR</sub> <sup>e</sup> (kDa)	Dispersity $(D)^f$	Yield (%) <sup>g</sup>
1	CssPy	22	10	2	100	10	3.4	1.09	49
2	CssPy	22	20	2	100	20	6.7	1.15	58
3	CssPy	22	30	2	93	28	9.0	1.17	69

4	CssPy	22	50	2	80	40	13.3	1.15	71
5	CssPy	22	100	2	70	70	23.5	1.25	85
6	CssPy	0	30	2	20	6	2.1	-	13
7	CssPy	0	30	4	47	14	4.7	-	27

<sup>a</sup>The initiator was 4-methylbenzyl alcohol, the solvent was anhydrous CH<sub>2</sub>Cl<sub>2</sub>, monomer was CssPy, and DBU was used as the catalyst with 5 mol% to monomers for all entries. <sup>b</sup>The concentration of monomer CssPy was 0.5 M. <sup>c</sup>Conversions were obtained from <sup>1</sup>H NMR spectra. <sup>d</sup>Degree of polymerization (DP) and <sup>e</sup> $M_{n,NMR}$  was estimated from integral ratios of the methylene protons connected to oxygen (protons 2 and 3) on the repeating units between 4.36 to 4.27 ppm with the methyl protons originating from the initiator on the α-chain end at 2.32 ppm (proton 13) based on <sup>1</sup>H NMR of final polymer products. <sup>f</sup>Dispersity was measured by SEC calibrated with poly(methyl methacrylate) standards. <sup>g</sup>Yield was calculated by dividing the actual amount of polymer Bn-PCssPy<sub>n</sub> obtained after purification by theoretical yield based on monomer conversion.

2.3. Kinetics study of the ROP of activated cyclic carbonates. The polymerization kinetics of pyridyl disulfide-containing cyclic carbonate monomer CssPy was investigated using a [M]<sub>0</sub>/[I]<sub>0</sub> ratio of 30 in anhydrous dichloromethane, initiated by 4-methylbenzyl alcohol and catalyzed by DBU (Figure 2). Time-dependent monomer conversions and polymer chain growth were monitored with <sup>1</sup>H NMR spectroscopy by collecting aliquots of the polymerization mixtures at different time intervals. The decrease of monomer concentration was calculated using the integration of methylene protons  $2_m$ ,  $2_m$ , and  $3_m$  at 4.70-4.19 ppm and those of polymers (protons  $2_p$  and  $3_p$  at 4.36-4.27 ppm) (Figure 2B). The  $M_n$  of polymers were calculated using <sup>1</sup>H NMR spectroscopy after purification by precipitating into diethyl ether-hexane solution (1/1, v/v) forthree times. A rapid ROP of the cyclic carbonate monomer was revealed in this kinetics study, which reached a remarkable 70% conversion within 30 min and more than 90% conversion within 120 min (Figure 2C and S13C). The kinetic plots of  $ln([M]_0/[M])$  were linearly dependent on reaction time (Figure 2C), indicating the polymerization of cyclic carbonate was a first-order reaction and the reaction rate was proportional to the monomer concentration. The linearity of  $M_n$  versus monomer conversion (Figure 2D) suggested that the

numbers of macromolecules in the reactions remained constant during the ring-opening polymerization, further demonstrating the controlled characteristics of the ROP of cyclic carbonate.

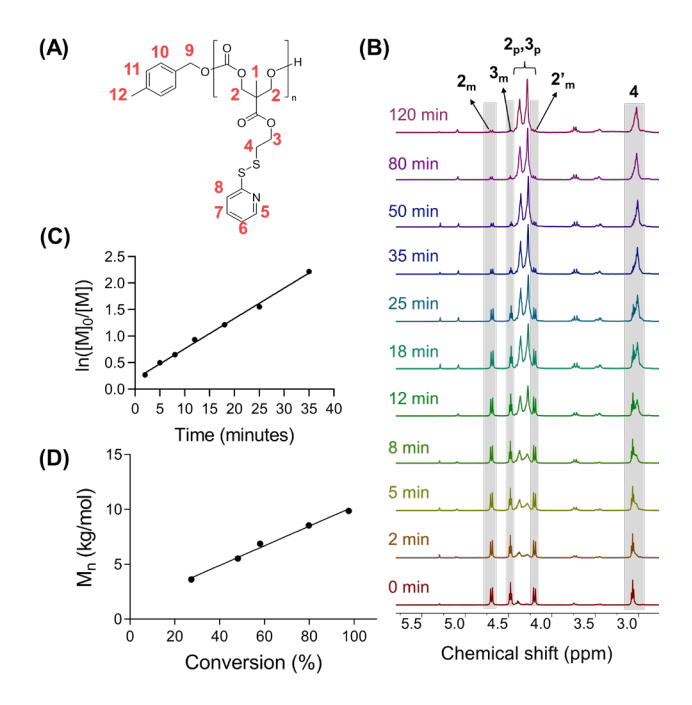


**Figure 2.** Kinetics study of the ROP of activated cyclic carbonate **CssPy** using DBU as the catalyst and 4-methylbenzyl alcohol as the initiator. (A) Chemical structure of **Bn-PCssPy**. (B) Characteristic <sup>1</sup>H NMR changes of the ROP of **CssPy** vs time in CDCl<sub>3</sub>. (C) Plots of monomer conversion (ln([M]<sub>0</sub>/[M]) vs time (0-35 min) calculated from <sup>1</sup>H NMR spectra. (D) Plots of  $M_n$  vs monomer conversion obtained from <sup>1</sup>H NMR spectra.

**2.4 Postmodification of polycarbonates** *via* **thiol-disulfide exchange reaction.** One of the most fascinating features of the responsive polycarbonate **Bn-PCssPy** is that the pyridine disulfide group is a highly efficient activated moiety for versatile modification *via* thiol exchange reaction which can be undertaken in most organic and aqueous solutions in a wide pH range

without the use of catalysts. Thus, the activated pyridyl disulfide pendent group of **Bn-PCssPy** enabled the facile postmodification to precisely tune its properties for biomedical applications. To validate the versatility of facile post-polymerization modification, thiols with different functionalities were subjected to conjugation with Bn-PCssPy including 2-(2methyoxyethoxy)ethanethiol as a model alkoxyl chain, positively-charged cysteamine hydrochloride, 3-mercaptopropionic acid, and zwitterionic homocysteine, to endow the polymer with different pendant functionalities and improved aqueous solubility (Scheme 2 and Table S2). Dichloromethane (CH<sub>2</sub>Cl<sub>2</sub>) and N,N-dimethylformamide (DMF) were the preferred solvents for these reactions owing to their good ability to solubilize **Bn-PcssPy**. To aid in the dissolution of the thiol reactant, methanol and HCl were added to improve the solubility of cysteamine hydrochloride and homocysteine in DMF, respectively. The reaction solutions changed their colors from colorless to yellow almost immediately after adding the thiol due to the production of 2-mercaptopyridine as a side product. To ensure complete conversion of pyridyl disulfides, an excess of thiols (2 equivalents to the disulfide group on polymers) was employed to react with **Bn-PcssPy** (50 mg/mL) for 24 hours at room temperature. The postmodified polymers were then purified by precipitating into hexane-diethyl ether mixture or dialysis against water. It was found almost 100% side chain conversions with up to 58% yields and were attained during our synthesis, as determined by the disappearance of the resonance peaks between 8.5 and 7.0 ppm and appearance of new peaks at around 3.0-4.5 ppm in <sup>1</sup>H NMR as a result of the removal of pyridine moieties and installation of new pendent groups (Figure S15-18). The mild reaction condition was compatible with the polycarbonate backbone without causing any degradation or crosslinking. Worth noting, the disulfide bonds were retained during the postmodification reaction, maintaining GSH responsiveness. The versatility of facile modification of pendant

chains highlights the advantage of our approach: one-step reaction under mild conditions with nearly complete conversion of functionalities, requiring no coupling agents and preserving of redox-response disulfide bonds. It is expected that multiple responsive functionalities could be potentially incorporated at the same time, allowing for fine-tuning of polymer properties with great potentials for various applications in the biomedical fields.

**Scheme 2.** Post-polymerization modification of **Bn-PCssPy** *via* thiol-disulfide exchange reaction to incorporate various functional pendent groups.

2.5 Amphiphilic PEG-*b*-polycarbonates for responsive drug delivery. We further designed a GSH-responsive polycarbonate novel APC-based drug delivery system where a highly cytotoxic drug mertansine (DM1) was conjugated to the polymer using the activated pendant side chains. DM1, a thiol containing maytansinoid, is a powerful tubulin inhibitor which can inhibit the assembly of microtubules.<sup>39-41</sup> Its antibody conjugate, trastuzumab emtansine (T-DM1), has been approved by FDA for the treatment of advanced cancers and applied for clinical trials since 2013.<sup>42-43</sup> Aside from the production and cost issues, T-DM1 also have issues with formulation instability, drug release, and serious adverse effects including nausea, musculoskeletal pain, hepatotoxicity, heart disease, and interstitial lung diseases.<sup>44</sup> Thus, biodegradable and biocompatible SDDSs that can safeguard DM1 during *in vivo* transportation

and release DM1 specifically in cancerous cells are promising strategies to achieve enhanced drug delivery with minimal cytotoxicity to healthy tissues.

To achieve this goal, we designed and synthesized amphiphilic diblock copolymer via the ROPs of activated disulfide bearing monomer CssPy using methoxy polyethylene glycol (mPEG-OH,  $M_n = 2000$  Da) as a macroinitiator and DBU as the organocatalyst (Figure 3). The synthesis of mPEG-b-PCssPy followed a similar synthetic approach as employed for Bn-PCssPy. After reacting at room temperature for 2 h, mPEG-b-PCssPy was purified by precipitating into the mixed solution of hexane-diethyl ether (1/1, v/v) with a yield of 59% and a dispersity of 1.26. DP of (n=12) and  $M_n$  (5.9 kDa) of mPEG-b-PCssPy were calculated from the <sup>1</sup>H NMR spectrum according to the integration of the methylene protons from polycarbonate block between 4.36 to 4.27 ppm and the methylene protons from the PEG initiator at 3.66 ppm (Figure S20). Eight equivalents of DM1 to polymer were used and all drug molecules were successfully conjugated to mPEG-b-PCssPy through the thiol-disulfide exchange reaction between the inherent thiol group of DM1 and pendant pyridyl disulfides (Figure 3). The resulting mPEG-b-PCssDM1 could also be purified by precipitating into the mixed solution of hexanediethyl ether (1/1, v/v) with a yield of 68% and a dispersity of 1.33 (Figure S19 and S21). The obvious peak shifting in SEC compared to mPEG-OH and mPEG-b-PCssPy indicated successful drug conjugation (Figure S19).

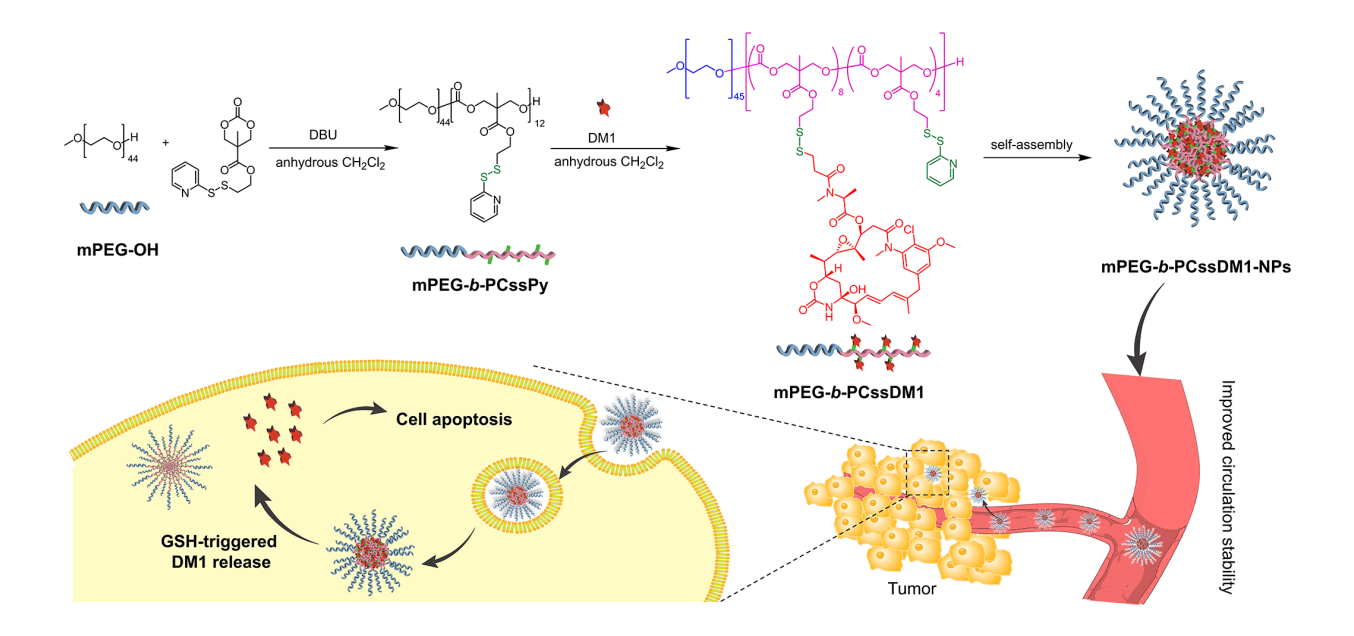


**Figure 3.** Schematic illustration of the synthesis of amphipathic diblock copolymer **mPEG-b-PCssDM1** and its self-assembled nanoparticles **mPEG-b-PCssDM1-NPs** for GSH-responsive DM1 release in cancer cells.

The obtained polymer-drug conjugate mPEG-b-PCssDM1 was amphiphilic where the drug conjugated APC block acted as the hydrophobic component and the mPEG chain acted as the hydrophilic segment. Due to the amphiphilic nature, mPEG-b-PCssDM1 could further self-assemble into nanoparticles (NPs) in the aqueous solution, where the conjugated DM1 was located in the nanoparticle core and mPEG served as the shell. Dynamic light scattering (DLS) analysis revealed that the hydrodynamic diameters of mPEG-b-PCssDM1-NPs were approximately 50 nm which is in agreement with dry-state substrate-adsorbed diameters of ~41 nm as measured by transmission electron microscopy (Figure 4A and Figure S22), a well-suited size to evade rapid clearance in blood circulation and cellular uptake. Additionally, the NPs exhibited negative zeta potentials of -24 mV (Figure 4B) which could help stabilize the NPs by creating electrostatic repulsion between them to prevent undesirable aggregation in aqueous

solutions. No apparent precipitation has been observed after storage in the refrigerator for several months, indicating superior colloidal and hydrolytic stability of the nanoparticles.

Glutathione (GSH), an essential intracellular antioxidant, plays significant roles in regulating redox status of cells, gene expression, cell proliferation, and apoptosis. 46-49 The overexpression of endogenous GSH has been deemed to be associated with the initiation and progression of various cancers, which can also be exploited to trigger targeted drug release in cancer cells. 50-52 *In vitro* GSH-responsive drug release was conducted by incubating mPEG-b-PCssDM1-NPs (10 μg/mL) in phosphate-buffered saline (PBS, pH 7.4) with different GSH concentrations (0, 50 nM, 2 mM, and 5 mM) at 37 °C. The cumulative DM1 release was monitored by highperformance liquid chromatography (HPLC) at predetermined time points. The time-dependent HPLC traces revealed an increasing sharp peak at 8.9 min for DM1, accompanied by a decreasing of a set of broad peaks between 10-13 min for polymer-DM1 conjugate, which signified the responsive release of DM1 molecules along with concurrent degradation of the polymer-DM1 conjugate (Figure 4C). The nanoparticle exhibited a relatively rapid drug release at the GSH concentration of 5 mM, achieving > 50% release of DM1 within 4 h and over 80 % release within 8 h (Figure 4D). The release was significantly decreased when the GSH concentration was lowered to 2 mM, and less than 50 % release of DM1 was observed within 10 hours. Furthermore, the nanoparticles remained stable at low GSH concentrations, for instance at 50 nM of GSH in PBS solution, no significant DM1 release was observed even after 12 hours. This ultrahigh sensitivity of GSH-concentration of mPEG-b-PCssDM1-NPs is highly desired since GSH is highly overexpressed and can reach millimolar levels in cancer cells and much lower concentrations in healthy cells, and extremely low levels during bloodstream circulation and in extracellular environment. 53-55 Therefore, the self-assembled polymer-drug conjugate is

expected to be stable during blood circulation and rapidly release DM1 in the cytosol of cancer cells, limiting systemic side effects and improving therapeutic efficacy.

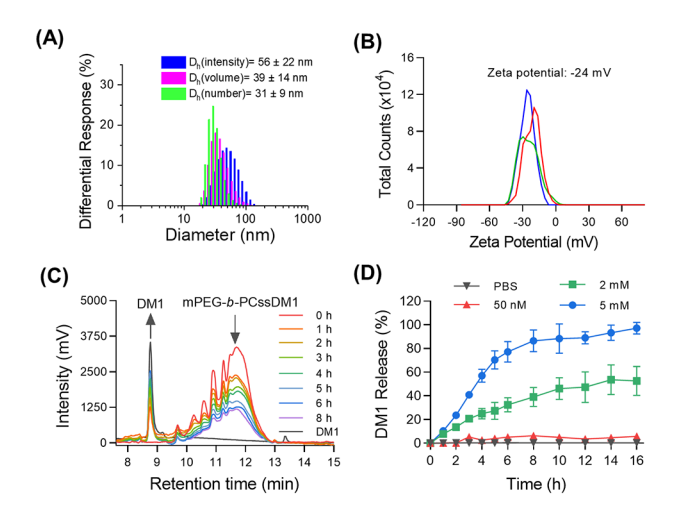


**Figure 4.** (A) The number-, volume-, and intensity-average hydrophobic diameters of **mPEG-b-PCssDM1-NPs** measured by DLS. (B) Zeta potentials of **mPEG-b-PCssDM1-NPs** measured by DLS. (C) The HPLC traces of **mPEG-b-PCssDM1-NPs** after incubation in PBS containing 5 mM GSH (pH 7.4, 37 °C) for different time. (D) The release profile of DM1 from **mPEG-b-PCssDM1-NPs** in PBS (pH 7.4, 37 °C) containing different GSH concentrations.

The anticancer potential of mPEG-b-PCssDM1-NPs was further investigated by measuring the cytotoxicity of mPEG-b-PCssDM1-NPs against cancerous cell lines and a healthy cell line. Different cell lines, including cancerous cell lines Hela (a human cervical cancer cell line), MCF-7 (a human adenocarcinoma cell line), and PANC-1 (a human pancreatic cancer cell line), and a healthy cell line hTERT-HPNE (hTERT-immortalized pancreatic epithelial cells) were treated with varying concentrations of free DM1 and mPEG-b-PCssDM1-NPs for 72 h at 37 °C. MTT assays were used to evaluate cell viability (Figure 5). As expected, DM1 was extremely toxic to all cell lines, including the healthy cell line with IC<sub>50</sub> ranging from 0.5-3.2 nM. The mPEG-b-PCssDM1-NPs remained potent to all these cancer cell lines, with increased IC<sub>50</sub> values ranging

from 7.2 nM to 37 nM (according to DM1 moieties concentrations), a ~10-fold lower cytotoxicity compared to free DM1 partly due to slower drug release. However, the cytotoxicity of mPEG-b-PCssDM1-NPs was significantly decreased in healthy hTERT-HPNE cells and the calculated IC50 value was increased over 140-fold compared to that of free DM1. In order to quantify the differential cytotoxicity of therapeutic agents, we calculated the ratio of IC50 value against the health hTERT-HPNE cell line vs different cancerous cells (Figure 5F). A greater ratio indicates a broader therapeutic window for the therapeutic agent. The significant greater ratio of mPEG-b-PCssDM1-NPs over that of DM1 demonstrated improved differential cytotoxicity against cancer cells over healthy cells, highlighting the great therapeutic potential of mPEG-b-PCssDM1-NPs in pancreatic cancer treatment. The difference was likely caused by the fast DM1 release kinetics under elevated GSH concentrations within the cancerous cells over healthy cells. Additionally, our polycarbonates exhibited negligible toxicities to Hela and MCF-7 cells after 24 h incubation (Figure S23) at applicable polymer concentrations (less than 0.1 mg/mL).

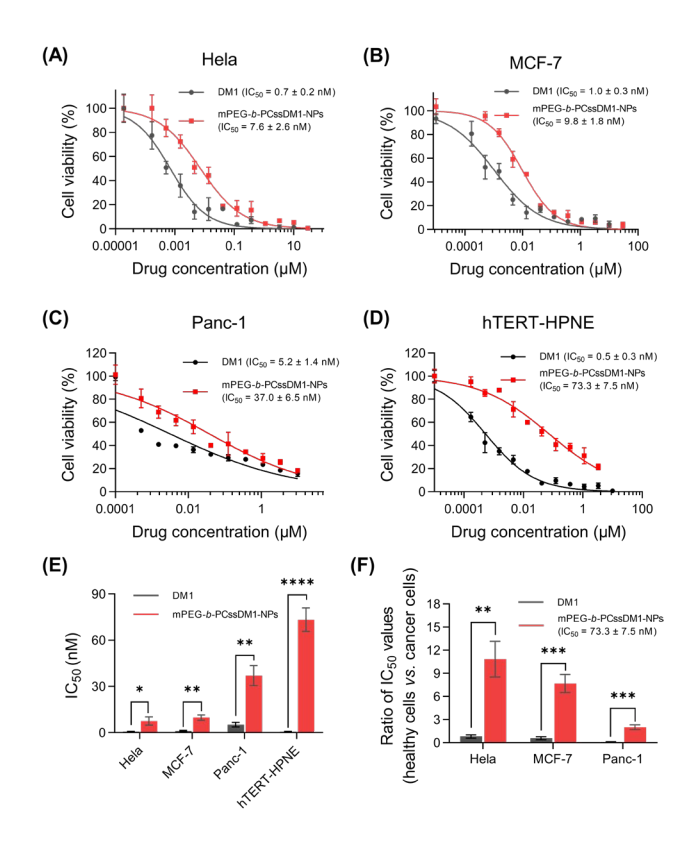


**Figure 5.** *In vitro* cytotoxicity of DM1 and **mPEG-***b***-PCssDM1-NPs** towards different cell lines (A) Hela, (B) MCF-7, (C) PANC-1, (D) hTERT-HPNE after 72 h-incubation at 37 °C and 5% CO<sub>2</sub>. (E) Calculated IC<sub>50</sub> values of DM1 and **mPEG-***b***-PCssDM1-NPs** towards different cells lines after 72 h-incubation. (D) Ratio of IC<sub>50</sub> values against the healthy hTERT-HPNE cells vs. different cancer cells after 72 h-incubation. Data are represented as means  $\pm$  standard deviation (n=3). \*p < 0.05, \*\*p < 0.01, \*\*\*p < 0.001 and \*\*\*\*p < 0.0001.

# 3. Conclusions

In summary, we have successfully established a versatile redox-responsive polycarbonate platform with pendant activated pyridyl disulfides which are readily to react with thiols under mild condition, demonstrating great potential for biomedical applications. The synthesis of the pyridyl disulfide-containing cyclic carbonate monomer was simple and efficient, and its

subsequent ring-opening polymerization yielded functional polycarbonates with a high yield, low dispersity, and easy purification. The ROPs of the activated monomer were a well-controlled and living polymerization as suggested by the polymerization kinetics and narrow molar mass distribution. Moreover, the pyridyl disulfide-containing polycarbonates could be easily postmodified to introduce different pendent groups *via* a highly efficient thiol-disulfide exchange reaction, providing a simple and versatile approach to fine-tuning polymer's physiochemical properties for applications in the biomedical field. As a proof of concept, we prepared an amphiphilic GSH-responsive polycarbonate-drug conjugate by initiating the cyclic carbonate monomer with mPEG-OH, followed by incorporating the anticancer drug DM1 *via* the thiol-disulfide exchange reaction. The self-assembled nanoparticles were a smart drug delivery system with GSH-triggered drug release specifically within cancer cells and a remarkable selective toxicity toward cancer cells over healthy cells, showcasing the exceptional promise of this GSH-responsive polycarbonate for biomedical applications.

### ASSOCIATED CONTENT

## **Supporting Information.**

The Supporting Information is available free of charge.

Materials, instruments, experimental procedures, and supplemental figures and tables, including <sup>1</sup>H NMR spectra, HRMS spectra, changes of cyclic carbonate monomer compared its precursors, kinetic study of the ROP of activated cyclic carbonate, thermogravimetric analysis and derivative thermogravimetric analysis spectra, SEC traces, and cytotoxicities of polycarbonate.

### **AUTHOR INFORMATION**

# **Corresponding Author**

\*Fuwu Zhang – Department of Chemistry, University of Miami, 1301 Memorial Drive, Coral Gables, Florida, 33146, United States; The Dr. John T. Macdonald Foundation Biomedical Nanotechnology Institute, University of Miami, Miami, FL, United States Email: fxz174@miami.edu

### **Authors**

**Xiao Zhang** – Department of Chemistry, University of Miami, 1301 Memorial Drive, Coral Gables, Florida, 33146, United States.

**Bowen Zhao** – Department of Chemistry, University of Miami, 1301 Memorial Drive, Coral Gables, Florida, 33146, United States.

**Shiwei Fu** – Department of Chemistry, University of Miami, 1301 Memorial Drive, Coral Gables, Florida, 33146, United States.

**Ronald S. Seruya** – Department of Chemistry, University of Miami, 1301 Memorial Drive, Coral Gables, Florida, 33146, United States.

**John F. Madey III** – Department of Chemistry, University of Miami, 1301 Memorial Drive, Coral Gables, Florida, 33146, United States.

**Eva Bukhryakova** – Department of Chemistry, University of Miami, 1301 Memorial Drive, Coral Gables, Florida, 33146, United States

# **Author Contributions**

The manuscript was written through contributions of all authors. All authors have given approval to the final version of the manuscript.

### **Notes**

The authors declare no competing financial interest.

## **ACKNOWLEDGMENT**

This work is supported by the National Science Foundation CAREER award under grant No. 2238812.

### **ABBREVIATIONS**

APC, aliphatic polycarbonate; bis-MPA, 2,2-bis(hydroxymethyl)propionic acid; GSH, glutathione; SDDS, drug delivery system; RAFT, reversible addition fragmentation chain transfer; ROP, ring-opening polymerization; DM1, mertansine; PEG, polyethylene glycol; NMR, nuclear magnetic resonance; DMF, dimethylformamide; TEM, transmission electron microscopy; DLS, dynamic light scattering; SEC, size-exclusion chromatography; HPLC, high-performance liquid chromatography.

### REFERENCES

- (1) Siegel, R. L.; Miller, K. D.; Wagle, N. S.; Jemal, A., Cancer Statistics, 2023. *CA Cancer J. Clin.* **2023**, *73* (1), 17-48.
- (2) Liao, Z. H.; Wong, S. W.; Yeo, H. L.; Zhao, Y., Smart Nanocarriers for Cancer Treatment: Clinical Impact and Safety. *Nanoimpact* **2020**, *20*. 100253-100262.
- (3) Zhong, L.; Li, Y. S.; Xiong, L.; Wang, W. J.; Wu, M.; Yuan, T.; Yang, W.; Tian, C. Y.; Miao, Z.; Wang, T. Q.; Yang, S. Y., Small Molecules in Targeted Cancer Therapy: Advances, Challenges, and Future Perspectives. *Signal Transduct. Tar.* **2021**, *6* (1), 201-248.
- (4) Zhang, C. Y.; Xu, C.; Gao, X. Y.; Yao, Q. Q., Platinum-Based Drugs for Cancer Therapy and Anti-Tumor Strategies. *Theranostics* **2022**, *12* (5), 2115-2132.

- (5) Debela, D. T.; Muzazu, S. G.; Heraro, K. D.; Ndalama, M. T.; Mesele, B. W.; Haile, D. C.; Kitui, S. K.; Manyazewal, T., New Approaches and Procedures for Cancer Treatment: Current Perspectives. *SAGE Open Med.* **2021**, *9*, 20503121211034366.
- (6) Lin, X.; Wu, J. H.; Liu, Y. P.; Lin, N. M.; Hu, J.; Zhang, B., Stimuli-Responsive Drug Delivery Systems for the Diagnosis and Therapy of Lung Cancer. *Molecules* **2022**, *27* (3), 948-961.
- (7) Hoop, M.; Mushtaq, F.; Hurter, C.; Chen, X. Z.; Nelson, B. J.; Pane, S., A Smart Multifunctional Drug Delivery Nanoplatform for Targeting Cancer Cells. *Nanoscale* **2016**, *8* (25), 12723-12728.
- (8) Taghizadeh, B.; Taranejoo, S.; Monemian, S. A.; Moghaddam, Z. S.; Daliri, K.; Derakhshankhah, H.; Derakhshani, Z., Classification of Stimuli-Responsive Polymers as Anticancer Drug Delivery Systems. *Drug Deliv.* **2015**, *22* (2), 145-155.
- (9) Liu, D.; Yang, F.; Xiong, F.; Gu, N., The Smart Drug Delivery System and Its Clinical Potential. *Theranostics* **2016**, *6* (9), 1306-1323.
- (10) Wang, Z. H.; Ye, Q. Z.; Yu, S.; Akhavan, B., Poly Ethylene Glycol (PEG)-Based Hydrogels for Drug Delivery in Cancer Therapy: A Comprehensive Review. *Adv. Healthc. Mater.* **2023**, *12* (18), 2300105-2300125.
- (11) Rana, A.; Adhikary, M.; Singh, P. K.; Das, B. C.; Bhatnagar, S., "Smart" Drug Delivery: A Window to Future of Translational Medicine. *Front. Chem.* **2023**, *10*, 1095598-1095631.
- (12) Liang, H.; Lu Q.; Yang, J.; Yu, G., Supermolecular Biomaterials for Cancer Immunotherapy. *Research* **2023**, *6*, 0211

- (13) Yang, J.; Yu, X.; Song, J. I.; Song Q.; Hall, S. C. L.; Yu, G.; Perrier, S. Aggregation-Induced Emission Featured Supramolecular Tubisomes for Imaging-Guided Drug Delivery. *Angew. Chem.* **2022**, *134*, e20211515208.
- (14) Yang, J.; Yu, G.; Sessler, J. L.; Shin, I.; Gale, P. A.; Huang, F. Artificial Transmembrane Ion Transporters as Potential Therapeutics. *Chem*, **2021**, *7*, 3256–3291.
- (15) Xu, J. W.; Feng, E.; Song, J., Renaissance of Aliphatic Polycarbonates: New Techniques and Biomedical Applications. *J. Appl. Polym. Sci.* **2014**, *131* (5), 10.1002/app.39822
- (16) Yu, W.; Maynard, E.; Chiaradia, V.; Arno, M. C.; Dove, A. P., Aliphatic Polycarbonates from Cyclic Carbonate Monomers and Their Application as Biomaterials. *Chem. Rev.* **2021**, *121* (18), 10865-10907.
- (17) Sanders, D. P.; Fukushima, K.; Coady, D. J.; Nelson, A.; Fujiwara, M.; Yasumoto, M.; Hedrick, J. L., A Simple and Efficient Synthesis of Functionalized Cyclic Carbonate Monomers Using a Versatile Pentafluorophenyl Ester Intermediate. *J. Am. Chem. Soc.* **2010**, *132* (42), 14724-14726.
- (18) Endo, T.; Kakimoto, K.; Ochiai, B.; Nagai, D., Synthesis and Chemical Recycling of A Polycarbonate Obtained by Anionic Ring-Opening Polymerization of A Bifunctional Cyclic Carbonate. *Macromolecules* **2005**, *38* (20), 8177-8182.
- (19) Jerome, C.; Lecomte, P., Recent Advances in the Synthesis of Aliphatic Polyesters by Ring-Opening Polymerization. *Adv. Drug. Deliver. Rev.* **2008**, *60* (9), 1056-1076.
- (20) AlSawaftah, N.; Pitt, W. G.; Husseini, G. A., Dual-Targeting and Stimuli-Triggered Liposomal Drug Delivery in Cancer Treatment. *ACS Pharmacol. Transl.* **2021**, *4* (3), 1028-1049.

- (21) Engler, A. C.; Chan, J. M. W.; Fukushima, K.; Coady, D. J.; Yang, Y. Y.; Hedrick, J. L. Polycarbonate-Based Brush Polymers with Detachable Disulfide-Linked Side Chains. *ACS Macro Lett.* **2013**, *2* (4), 332-336.
- (22) Riahinezhad, H.; Kerr-Dini, N.; Amsden, B. G. Degradation of Poly(vinyl sulfone carbonate) in Aqueous Media. *Polym. Degrad. Stab.* **2023**, *216*, 110472-110481.
- (23) Yoon, J. A.; Kamada, J.; Koynov, K.; Mohin, J.; Nicolay, R.; Zhang, Y. Z.; Balazs, A. C.; Kowalewski, T.; Matyjaszewski, K., Self-Healing Polymer Films Based on Thiol-Disulfide Exchange Reactions and Self-Healing Kinetics Measured Using Atomic Force Microscopy. *Macromolecules* **2012**, *45* (1), 142-149.
- (24) Zhang, P.; Wu, J. L.; Xiao, F. M.; Zhao, D. J.; Luan, Y. X., Disulfide Bond Based Polymeric Drug Carriers for Cancer Chemotherapy and Relevant Redox Environments in Mammals. *Med. Res. Rev.* **2018**, *38* (5), 1485-1510.
- (25) Quinn, J. F.; Whittaker, M. R.; Davis, T. P., Glutathione Responsive Polymers and Their Application in Drug Delivery Systems. *Polym. Chem.-Uk* **2017**, *8* (1), 97-126.
- (26) Zhang, D.; Li, L.; Ji, X. H.; Gao, Y. H., Intracellular GSH-Responsive Camptothecin Delivery Systems. *New J. Chem.* **2019**, *43* (47), 18673-18684.
- (27) Zhang, F. W.; Ni, Q. Q.; Jacobson, O.; Cheng, S. Y.; Liao, A.; Wang, Z. T.; He, Z. M.; Yu, G. C.; Song, J. B.; Ma, Y.; Niu, G.; Zhang, L. J.; Zhu, G. Z.; Chen, X. Y., Polymeric Nanoparticles with a Glutathione-Sensitive Heterodimeric Multifunctional Prodrug for In Vivo Drug Monitoring and Synergistic Cancer Therapy. *Angew. Chem. Int. Ed.* **2018**, *57* (24), 7066-7070.

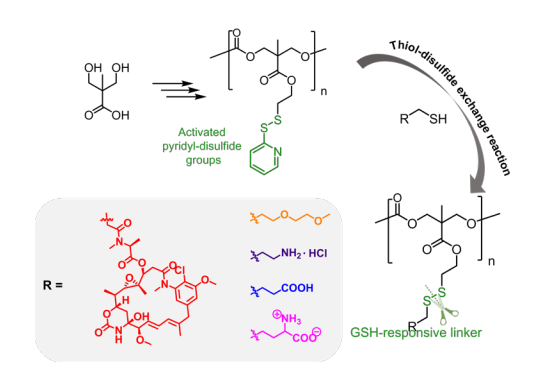
- (28) Bulmus, V.; Woodward, M.; Lin, L.; Murthy, N.; Stayton, P.; Hoffman, A., A New pH-responsive And Glutathione-Reactive, Endosomal Membrane-Disruptive Polymeric Carrier for Intracellular Delivery of Biomolecular Drugs. *J. Control. Release* **2003**, *93* (2), 105-120.
- (29) Zhang, W. J.; Hong, C. Y.; Pan, C. Y., Fabrication of Reductive-Responsive Prodrug Nanoparticles with Superior Structural Stability by Polymerization-Induced Self-Assembly and Functional Nanoscopic Platform for Drug Delivery. *Biomacromolecules* **2016**, *17* (9), 2992-2999.
- (30) Dong, S. X.; Sun, Y.; Liu, J.; Li, L.; He, J. L.; Zhang, M. Z.; Ni, P. H., Multifunctional Polymeric Prodrug with Simultaneous Conjugating Camptothecin and Doxorubicin for pH/Reduction Dual-Responsive Drug Delivery. *ACS Appl. Mater. Inter.* **2019**, *11* (9), 8740-8748.
- (31) Gao, J. J.; Dutta, K.; Zhuang, J. M.; Thayumanavan, S., Cellular- and Subcellular-Targeted Delivery Using a Simple All-in-One Polymeric Nanoassembly. *Angew. Chem. Int. Ed.* **2020,** *59* (52), 23466-23470.
- (32) Schäfer, O.; Huesmann, D.; Barz, M., Poly(S-ethylsulfonyl-L-cysteines) for Chemoselective Disulfide Formation. *Macromolecules* **2016**, *49* (21), 8146-8153.
- (33) Schäfer, O.; Huesmann, D.; Muhl, C.; Barz, M., Rethinking Cysteine Protective Groups: S-Alkylsulfonyl-L-Cysteines for Chemoselective Disulfide Formation. *Chem.-Eur. J.* **2016**, *22* (50), 18085-18091.
- (34) Cotarca, L.; Geller, T.; Répási, J., Bis(trichloromethyl)carbonate (BTC, Triphosgene): A Safer Alternative to Phosgene? *Org. Process Res. Dev.* **2017**, *21* (9), 1439-1446.

- (35) Baki, Z. A.; Dib, H.; Sahin, T., Overview: Polycarbonates via Ring-Opening Polymerization, Differences between Six- and Five-Membered Cyclic Carbonates: Inspiration for Green Alternatives. *Polymers.* **2022**, *14* (10), 2031-2050.
- (36) Azechi, M.; Matsumoto, K.; Endo, T., Anionic Ring-opening Polymerization of a Five-membered Cyclic Carbonate Having a Glucopyranoside Structure. *J. Polym. Sci. Pol. Chem.* **2013**, *51* (7), 1651-1655.
- (37) Su, W.-F., Ring-Opening Polymerization. In *Principles of Polymer Design and Synthesis*, Springer Berlin Heidelberg: Berlin, Heidelberg, 2013; pp 267-299.
- (38) Wright, K. J.; Badwaik, V. D.; Samaddar, S.; Hyun, S. H.; Glauninger, K.; Eom, T.; Thompson, D. H., Organocatalytic Synthesis and Evaluation of Polycarbonate Pendant Polymer:beta-Cyclodextrin-Based Nucleic Acid Delivery Vectors. *Macromolecules* **2018**, *51* (3), 670-678.
- (39) Gao, S.; Zhang, W. Z.; Wang, R. J.; Hopkins, S. P.; Spagnoli, J. C.; Racin, M.; Bai, L.; Li, L.; Jiang, W.; Yang, X. Y.; Lee, C.; Nagata, K.; Howerth, E. W.; Handa, H.; Xie, J.; Ma, Q. J.; Kumar, A., Nanoparticles Encapsulating Nitrosylated Maytansine To Enhance Radiation Therapy. *ACS Nano* **2020**, *14* (2), 1468-1481.
- (40) White, B. H.; Whalen, K.; Kriksciukaite, K.; Alargova, R.; Yeung, T. A.; Bazinet, P.; Brockman, A.; DuPont, M.; Oller, H.; Lemelin, C. A.; Soo, P. L.; Moreau, B.; Perino, S.; Quinn, J. M.; Sharma, G.; Shinde, R.; Sweryda-Krawiec, B.; Wooster, R.; Bilodeau, M. T., Discovery of an SSTR2-Targeting Maytansinoid Conjugate (PEN-221) with Potent Activity in Vitro and in Vivo. *J. Med. Chem.* **2019**, *62* (5), 2708-2719.
- (41) Widdison, W. C.; Wilhelm, S. D.; Cavanagh, E. E.; Whiteman, K. R.; Leece, B. A.; Kovtun, Y.; Goldmacher, V. S.; Xie, H. S.; Steeves, R. M.; Lutz, R. J.; Zhao, R.; Wang, L. T.;

- Blättler, W. A.; Chari, R. V. J., Semisynthetic Maytansine Analogues for the Targeted Treatment of Cancer. *J. Med. Chem.* **2006**, *49* (14), 4392-4408.
- (42) Chudasama, V.; Maruani, A.; Caddick, S., Recent Advances in the Construction of Antibody-Drug Conjugates. *Nat. Chem.* **2016**, *8* (2), 113-118.
- (43) Lambert, J. M.; Chari, R. V. J., Ado-trastuzumab Emtansine (T-DM1): An Antibody-Drug Conjugate (ADC) for HER2-Positive Breast Cancer. *J. Med. Chem.* **2014**, *57* (16), 6949-6964.
- (44) Zhong, P.; Zhang, J.; Deng, C.; Cheng, R.; Meng, F. H.; Zhong, Z. Y., Glutathione-Sensitive Hyaluronic Acid-SS-Mertansine Prodrug with a High Drug Content: Facile Synthesis and Targeted Breast Tumor Therapy. *Biomacromolecules* **2016**, *17* (11), 3602-3608.
- (45) Hoshyar, N.; Gray, S.; Han, H. B.; Bao, G., The Effect of Nanoparticle Size on in vivo Pharmacokinetics and Cellular Interaction. *Nanomedicine-Uk* **2016**, *11* (6), 673-692.
- (46) Mochizuki, A.; Saso, A.; Zhao, Q. C.; Kubo, S.; Nishida, N.; Shimada, I., Balanced Regulation of Redox Status of Intracellular Thioredoxin Revealed by in-Cell NMR. *J. Am. Chem. Soc.* **2018**, *140* (10), 3784-3790.
- (47) Li, Q. J.; Chen, M.; Chen, D. Y.; Wu, L. M., One-Pot Synthesis of Diphenylalanine-Based Hybrid Nanospheres for Controllable pH- and GSH-Responsive Delivery of Drugs. *Chem. Mater.* **2016**, *28* (18), 6584-6590.
- (48) Ryu, J. H.; Chacko, R. T.; Jiwpanich, S.; Bickerton, S.; Babu, R. P.; Thayumanavan, S., Self-Cross-Linked Polymer Nanogels: A Versatile Nanoscopic Drug Delivery Platform. *J. Am. Chem. Soc.* **2010**, *132* (48), 17227-17235.
- (49) Morozumi, A.; Kamiya, M.; Uno, S. N.; Umezawa, K.; Kojima, R.; Yoshihara, T.; Tobita, S.; Urano, Y., Spontaneously Blinking Fluorophores Based on Nucleophilic

- Addition/Dissociation of Intracellular Glutathione for Live-Cell Super-resolution Imaging. *J. Am. Chem. Soc.* **2020,** *142* (21), 9625-9633.
- (50) Kennedy, L.; Sandhu, J. K.; Harper, M. E.; Cuperlovic-Culf, M., Role of Glutathione in Cancer: From Mechanisms to Therapies. *Biomolecules* **2020**, *10* (10), 1429-1456.
- (51) Hakuna, L.; Doughan, B.; Escobedo, J. O.; Strongin, R. M., A Simple Assay for Glutathione in Whole Blood. *Analyst* **2015**, *140* (10), 3339-3342.
- (52) Ballatori, N.; Krance, S. M.; Notenboom, S.; Shi, S. J.; Tieu, K.; Hammond, C. L., Glutathione Dysregulation and the Etiology and Progression of Human Diseases. *Biol. Chem.* **2009**, *390* (3), 191-214.
- (53) Circu, M. L.; Aw, T. Y., Glutathione and Modulation of Cell Apoptosis. *BBA-Mol. Cell Res.* **2012**, *1823* (10), 1767-1777.
- (54) Yu, G. C.; Zhao, X. L.; Zhou, J.; Mao, Z. W.; Huang, X. L.; Wang, Z. T.; Hua, B.; Liu, Y. J.; Zhang, F. W.; He, Z. M.; Jacobson, O.; Gao, C. Y.; Wang, W. L.; Yu, C. Y.; Zhu, X. Y.; Huang, F. H.; Chen, X. Y., Supramolecular Polymer-Based Nanomedicine: High Therapeutic Performance and Negligible Long-Term Immunotoxicity. *J. Am. Chem. Soc.* **2018**, *140* (25), 8005-8019.
- (55) Yu, G. C.; Yang, Z.; Fu, X.; Yung, B. C.; Yang, J.; Mao, Z. W.; Shao, L.; Hua, B.; Liu, Y. J.; Zhang, F. W.; Fan, Q. L.; Wang, S.; Jacobson, O.; Jin, A.; Gao, C. Y.; Tang, X. Y.; Huang, F. H.; Chen, X. Y., Polyrotaxane-Based Supramolecular Theranostics. *Nat. Commun.* **2018**, *9*, 766-778.
- (56) Lin, Y. N.; Khan, S.; Song, Y.; Dong, M.; Shen, Y. D.; Tran, D. K.; Pang, C.; Zhang, F. W.; Wooley, K. L., A Tale of Drug-Carrier Optimization: Controlling Stimuli Sensitivity via Nanoparticle Hydrophobicity through Drug Loading. *Nano Lett.* **2020**, *20* (9), 6563-6571.

# For Table of Contents Only



A rapid and versatile strategy to synthesize glutathione-responsive polycarbonates through the controlled ring-opening polymerization of cyclic carbonates with activated disulfides is reported, where the pendant activated pyridyl disulfides are readily to react with thiols under mild conditions, demonstrating great potential for biomedical applications.